

RESEARCH ARTICLE

Iron nanoparticle-labeled murine mesenchymal stromal cells in an osteoarthritic model persists and suggests anti-inflammatory mechanism of action

Amanda M. Hamilton¹✉, Wing-Yee Cheung²✉, Alejandro Gómez-Aristizábal², Anirudh Sharma², Sayaka Nakamura², Amélie Chaboureau², Shashank Bhatt², Razieh Rabani^{2,3}, Mohit Kapoor^{2,3,4}, Paula J. Foster^{1,5}, Sowmya Viswanathan^{2,3,6,7}✉*

1 Imaging Research Laboratories, Robarts Research Institute, London, ON, Canada, **2** The Arthritis Program, Toronto Western Hospital, Toronto, ON, Canada, **3** Division of Genetics and Development, Krembil Research Institute, University Health Network, Toronto, ON, Canada, **4** Department of Surgery, Department of Laboratory Medicine and Pathobiology, University of Toronto, Toronto, ON, Canada, **5** Department of Medical Biophysics, Schulich School of Medicine and Dentistry, Western University, London, ON, Canada, **6** Institute of Biomaterials and Biomedical Engineering, University of Toronto, Toronto, ON, Canada, **7** Department of Medicine, University of Toronto, Toronto, ON, Canada

✉ These authors contributed equally to this work.

* sowmya.viswanathan@uhnresearch.ca



OPEN ACCESS

Citation: Hamilton AM, Cheung W-Y, Gómez-Aristizábal A, Sharma A, Nakamura S, Chaboureau A, et al. (2019) Iron nanoparticle-labeled murine mesenchymal stromal cells in an osteoarthritic model persists and suggests anti-inflammatory mechanism of action. PLoS ONE 14(12): e0214107. <https://doi.org/10.1371/journal.pone.0214107>

Editor: Marlène Wiart, CarMeN U1060 Inserm, FRANCE

Received: March 5, 2019

Accepted: November 14, 2019

Published: December 3, 2019

Copyright: © 2019 Hamilton et al. This is an open access article distributed under the terms of the [Creative Commons Attribution License](https://creativecommons.org/licenses/by/4.0/), which permits unrestricted use, distribution, and reproduction in any medium, provided the original author and source are credited.

Data Availability Statement: All relevant data are within the manuscript and its Supporting Information files.

Funding: This study received peer review funding from the Ontario Institute for Regenerative Medicine and Stem Cell Network and funding from The Arthritis Society (15-321) and Stem Cell Network (Clinical Trial Impact grant # 8). The funders had no role in study design, data collection

Abstract

Osteoarthritis (OA) is characterized by cartilage degradation and chronic joint inflammation. Mesenchymal stem cells (MSCs) have shown promising results in OA, but their mechanism of action is not fully understood. We hypothesize that MSCs polarize macrophages, which are strongly associated with joint inflammation to more homeostatic sub-types. We tracked ferumoxytol (Feraheme™, iron oxide nanoparticle)-labeled murine MSCs (Fe-MSCs) in murine OA joints, and quantified changes to joint inflammation and fibrosis. 10-week-old C57BL/6 male mice (n = 5/group) were induced to undergo osteoarthritis by destabilization of medial meniscus (DMM) or sham surgery. 3 weeks post-surgery, mice were injected intra-articularly with either fluorescent dye-(DiR) labeled or DiR-Fe-MSC or saline to yield 4 groups (n = 5 per group for each timepoint [1, 2 and 4 weeks]). 4 weeks after injection, mice were imaged by MRI, and scored for i) OARSI (Osteoarthritis Research Society International) to determine cartilage damage; ii) immunohistochemical changes in iNOS, CD206, F4/80 and Prussian Blue/Sca-1 to detect pro-inflammatory, homeostatic and total macrophages and ferumoxytol -labeled MSCs respectively, and iii) Masson's Trichrome to detect changes in fibrosis. Ferumoxytol-labeled MSCs persisted at greater levels in DMM vs. SHAM-knee joints. We observed no difference in OARSI scores between MSC and vehicle groups. Sca-1 and Prussian Blue co-staining confirmed the ferumoxytol label resides in MSCs, although some ferumoxytol label was detected in proximity to MSCs in macrophages, likely due to phagocytosis of apoptotic MSCs, increasing functionality of these macrophages through MSC efferocytosis. MRI hypertintensity scores related to fluid edema decreased in MSC-treated vs. control animals. For the first time, we show that MSC-treated mice had increased ratios of %CD206⁺: %F4/80⁺ (homeostatic macrophages) (p<0.05),

and analysis, decision to publish, or preparation of the manuscript.

Competing interests: The authors have read the journal's policy and the authors of this manuscript have the following competing interests: SV owns a regulatory consulting company. There are no patents, products in development or marketed products associated with this research to declare. This does not alter our adherence to PLOS ONE policies on sharing data and materials.

and decreased ratios of %iNOS⁺: %F4/80⁺ macrophages ($p < 0.01$), supporting our hypothesis that MSCs may modulate synovial inflammation.

Introduction

Osteoarthritis (OA) is a common joint disease affecting 1 in 10 Canadians and is expected to increase to 1 in 4 by 2040. Similarly, the number of adults in the US with doctor-diagnosed arthritis is also expected to increase to 25.9% of all adults by 2040.[1] It is a lasting condition in which cartilage breaks down, causing bones to rub against each other, resulting in stiffness, pain and loss of joint movement. Currently, there are few effective treatments available for patients suffering from osteoarthritis. Mesenchymal Stromal Cells (MSCs) are cells that can be obtained from bone marrow and other tissues. Early clinical data shows improvements in cartilage volume and quality [2–7] and secretion of immunomodulatory factors. Our pioneering Canadian trial (NCT02351011, clinicaltrials.gov) using autologous bone-marrow-derived MSCs showed significant improvement in symptoms and quality of life relative to baseline in osteoarthritic patients; for the first time, we showed clinically that MSCs reduced synovial joint levels of pro-inflammatory macrophages, a potent inflammatory mediator, suggestive of a possible mechanism of action [8]. Macrophages are the most prevalent immune cell in OA joints [9], are elevated in OA compared to healthy joints [10], and contribute to synovial inflammation and fibrosis, characteristic of OA.

Understanding the immediate post-transplant joint environment by visualizing and monitoring localization and persistence of MSCs in a direct, non-invasive, longitudinal manner will address a major barrier in evaluating the success of MSC therapies in OA. Although early clinical trial results with MSCs are promising, unanswered questions regarding dosing, timing, frequency, interaction with macrophages, and mechanism of action of MSC persist.

Previously MSCs have been imaged in animal models using superparamagnetic iron oxide nanoparticles (SPIO) such as such as ferumoxides and ferucarbotran (i.e. Feridex™, Endorem® and Resovist™) because of their ease of use in stem cells, greater sensitivity for MR imaging compared to other contrast agents including gadolinium and CellSense, and lack of requirement for specialized multinuclear MRI systems for visualization. Ultrasmall SPIOs (i.e. ferumoxytol or Feraheme™) are introduced into cells by endocytosis and require transfection protocols using protamine sulfate and heparin [11]. Ferumoxytol has been clinically-approved by Health Canada and the Food and Drug Administration (FDA) for treatment of anemia in chronic-kidney disease patients, making it an attractive cell tracking agent via an off-label use.

Adipose-tissue MSCs have previously been labeled by endocytosis *in vitro* with ferumoxytol using protamine sulfate and feasibility of imaging *in vitro* and *in vivo* in rats models of osteochondral defects has been shown [12]. Other studies have also imaged MSCs labeled with other iron-nanoparticles and demonstrated persistence out to 5 weeks [13] in Hartley strain guinea pigs, and persistence out to 6 months in immunosuppressed NOD-SCID mice [14].

In this study, we attempted to demonstrate feasibility of labeling and MRI tracking of murine MSCs in a murine joint model of mildly inflammatory osteoarthritis that is clinically translatable and relevant. This study serves as a pre-requisite for subsequent clinical translation involving ferumoxytol-labeling of human MSCs intra-articularly injected into knee OA patients. Importantly, we wanted to identify a putative anti-inflammatory mechanism of action of MSCs, specifically through polarization of monocytes/macrophages in the arthritic joint. Monocytes/macrophages are the most prominent immune effects in OA and their levels

correlate with OA severity, which we have recently also correlated with patient-reported pain and symptoms [15].

Materials and methods

Human subject research

The Research Ethics Board from the University Health Network has approved the collection of the bone marrow used to generate the MSCs from human participants (REB# 06–0446) in this study. Consent was always obtained in a written form.

Animal research

This study was carried out in strict accordance with the standards of the Canadian Council of Animal Care. All animal work was approved by the Animal Use Subcommittee of the University Council on Animal Care at the University of Western Ontario (Protocol Number 2014–044). All efforts were made to minimize any animal suffering. Mice were anesthetized by inhalant isoflurane for surgical, injection and imaging procedures. At end point mice were humanely euthanized by inhalant isoflurane overdose.

Cell isolation

Mouse bone marrow stromal mesenchymal cells (BM-MSCs) were isolated from mouse long bones. Briefly, bone marrow was flushed out of mouse long bones (mouse tibiae, femurs), and were cultured in low glucose DMEM, supplemented with 10% FBS and Glutamine for less than 14 days. For *in vitro* cell labeling comparisons human BM-MSCs were isolated from bone marrow aspirate of consenting donors as previously described [8].

Animals

10 week-old C57BL/6 male mice (n = 5/group, Jackson Laboratories) were used for our studies. Mice underwent surgery (destabilization of medial meniscus (DMM) or sham surgery) and injected with either fluorescent dye-(DiR) labeled or DiR-ferumoxylol-labeled (DiR-Fe) mesenchymal stem cells (MSC) or saline (control), and were thus separated into 4 treatment groups: i) DMM+Saline; ii) DMM+DiR+Fe-MSC; iii) DMM+DiR MSC; iv) SHAM+DiR+Fe-MSC and saline in contralateral knee (Fig 1). All mice were fed ad libitum and were allowed to roam freely in cages throughout the study.

Surgical induction of instability

DMM surgery was performed as described by Glasson et al. [16]. Briefly, mice were induced with 2% isoflurane, and their right knees were shaved and prepped with iodine. At 90 degrees of flexion, the joint line was identified using a straight sharp tip micro probe (0.025 mm) facilitating the establishment of a medial para-patellar intra-articular port. A 3 mm skin incision was made over the medial portal using a knife with a number 10 blade. Following this, the capsule was incised in line with the skin incision medial to the patellar ligament. With the help of a microcurette (0.5 mm), the fat pad was dissected and the medial meniscotibial ligament (MRTL) was exposed. The MRTL is a translucent transverse band that connects the medial meniscus (MM) to the tibial plateau. Under direct vision, the MRTL was incised using a straight tip vannas spring scissors (0.075 mm). Care was taken not to damage the cartilage or other soft tissue structures. During the destabilization, bleeding encountered was controlled with direct pressure using absorption sponges. The destabilization was confirmed using a probe against the freely mobile medial meniscus. The capsule and skin were then sutured (8–0).

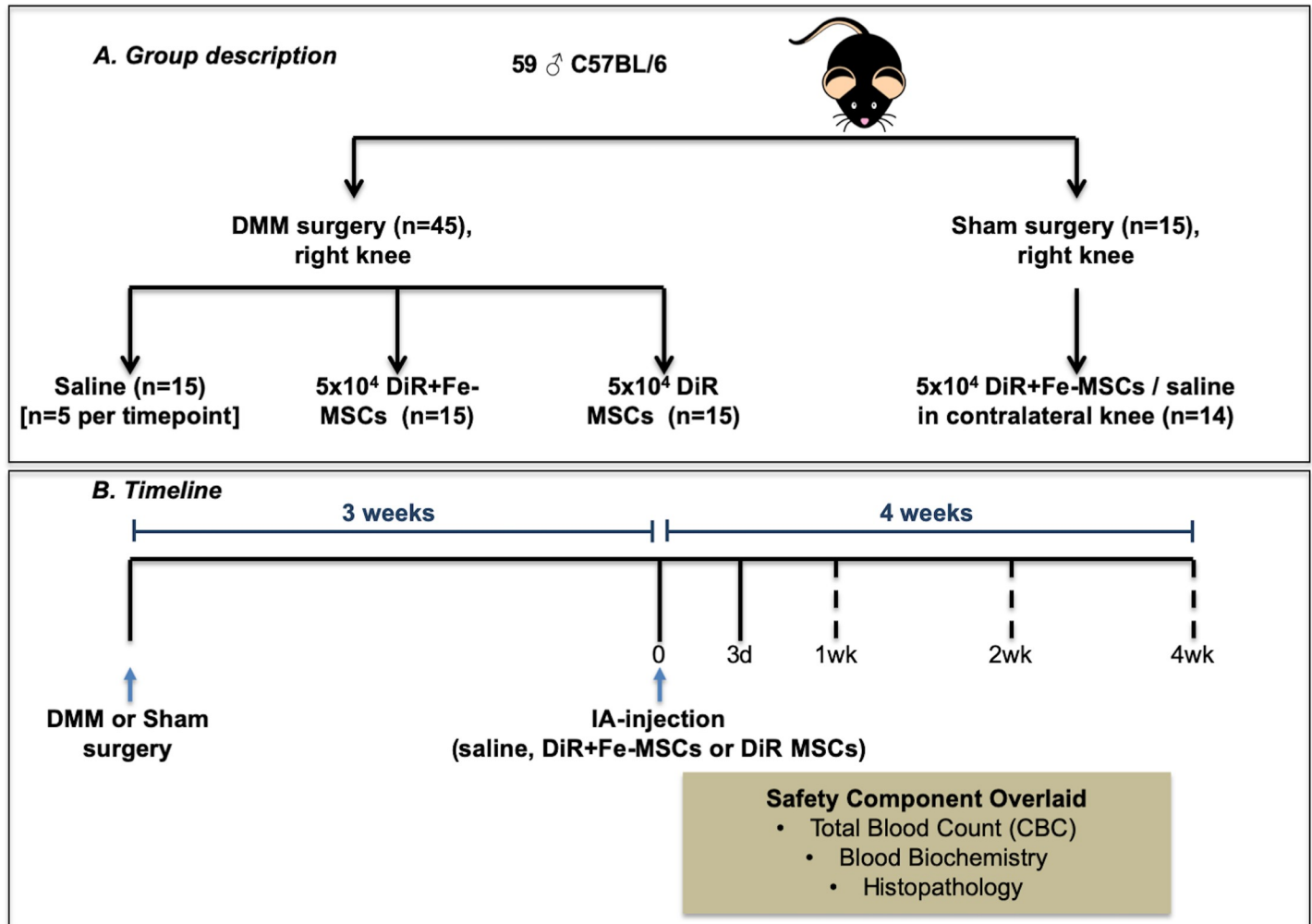


Fig 1. Experimental schematic of the DMM model. (A) Group description: 10 week old male C57BL/6 mice were subjected to DMM or SHAM surgery. 3 weeks post-DMM surgery, mice were injected intra-articularly with saline, DiR+ferumoxytol-labeled MSCs (DiR+Fe-MSCs), or only DiR-labeled MSCs (DiR-MSCs) in the right knees (n = 5/timepoint). SHAM operated mice were injected with MSCs in right knees, and saline on left knees. (n = 4 for 1 week, n = 5 for 2 and 4 week timepoints). DiR: 1,1'-Dioctadecyl-3,3,3',3'-Tetramethylindotricarbocyanine Iodide. (B) Timeline: Mice were assessed for total blood count, blood biochemistry, histopathology and MSC persistence in knee joints via MRI (On day 0 and day 3, and 1, 2 or 4 weeks post-injection). Dotted lines indicate that only one of the timepoints were selected for MRI.

<https://doi.org/10.1371/journal.pone.0214107.g001>

Buprenorphine (0.2 mg/mL, Indivior) was injected subcutaneously at the time of surgery and 24 hours post-surgery for pain maintenance. Mice were allowed to roam freely in their cages after surgery and monitored closely for post-surgical complications.

Cell labeling and injection

A subset of research animals (DMM and sham) received ferumoxytol-labeled MSC. Prior to intra-articular injection, MSCs were incubated for 2h with 50 µg Fe/mL ferumoxytol (Feraheme™; AMAG Pharmaceuticals Inc., Waltham, MA, USA) as per Thu et al in serum-free DMEM containing 3 U/mL heparin and 60 mg/mL protamine sulfate at 37°C, 5% CO₂ [11]. After this initial incubation, cells were supplemented with complete low glucose DMEM (containing 10% FBS) and further incubated at 37°C, 5% CO₂ overnight. After labeling, cells underwent sequential PBS washing before and after dissociation. All cells (Fe-MSCs and

unlabeled MSCs) were stained with the lipophilic fluorescent dye DiR (also called DiIC18(7), full chemical name: 1,1'-Dioctadecyl-3,3,3',3'-Tetramethylindotricarbocyanine Iodide) for 30 minutes and then washed three times with PBS before quantification. DiR is a lipophilic, near-infrared fluorescent cyanine dye that causes no cytotoxicity to stained cells when used at the concentration employed for this study. As this was primarily a cell tracking study, DiR was used to track all MSC (ferumoxytol-labeled and unlabeled) by fluorescence imaging. Without this label, which is not cytotoxic, we would not have been able to track cells. Cell viability was assessed by trypan blue exclusion assay, and cells were subsequently intra-articularly injected into mice in accordance to their respective groups (Fig 1).

Intra-articular knee injections

Mice were induced with 2% isoflurane, and their knees were depilated, prepped and positioned as in the DMM surgery. The patellar ligament was identified as a pearl-white vertical band. Using a 10 μ L Hamilton Syringe with custom 30G needle, the joint line was identified, and the needle was inserted along the medial border of the patellar ligament, keeping it in line with the joint line, slowly advancing it till loss of resistance was appreciated. Following this, the plunger was slowly pushed to deliver 4 μ L of DiR+Fe-MSCs or DiR-MSCs (5×10^4 cells) into the joint space. Once the MSCs were delivered, the needle was removed, and the knee joint was flexed and extended slowly. Saline was used as a vehicle control treatment.

Magnetic resonance imaging and analysis

All MRI examinations were performed using a 3 Tesla (T) GE Discovery MR750 whole-body clinical MR scanner with a custom-build high-performance gradient insert coil (maximum gradient strength = 500 mT/m and peak slew rate = 3000 T/m/s) and a custom solenoid radio-frequency mouse body coil (4 cm long, 3 cm diameter). Mice were anaesthetized with 2% isoflurane. Whole-body mouse images were acquired with the following three dimensional balance steady state free precession (3D bSSFP) imaging parameters: 200 μ m isotropic spatial resolution, with a 5-cm field of view (FOV) and 250 x 250 image matrix and a 200 μ m slice thickness; phase FOV = 0.5; repetition time/echo time (TR/TE): 6.3/3.152; flip angle = 35°; bandwidth = ± 31.25 kHz; eight phase cycles; number of excitations = 2; scan time = 34min.

Mice were imaged three times during the course of the experiment: on the day of cell delivery (day 0), 3 days post- and either 1, 2 or 4 weeks post-cell delivery. Images were viewed and analyzed using the open-source DICOM viewer OsiriX (Pixmeo, Switzerland). Void volumes were measured via manual hand tracing and volume calculation algorithms (Osirix) to assess presence of MSCs in joint space over time. MR images of DMM surgical knees were also scored for suspected evidence of inflammation. Scoring was conducted on a scale of 1 to 5 where 1 indicated no evidence of inflammation (resemblance to control non-surgical knees) and 5 indicated clear evidence of inflammation including increased total knee volume and hyperintense signal of tissue surrounding the knee joint.

Viability

Viability of DiR-labeled and DiR-Fe-labeled murine MSCs (n = 4) and human MSCs (n = 3) was assessed by Trypan blue dye exclusion using ViCell (Beckman Coulter).

Lineage differentiation

Unlabeled and ferumoxytol-labeled human and murine MSCs were tested for chondrogenic and osteogenic differentiation potential using MesenCult (StemCell Technologies)

differentiation as per manufacturer's instructions. Unlabeled and ferumoxytol-labeled human MSCs were tested for differentiation potential using StemPro differentiation kits (Life technologies) for chondrogenic and osteogenic differentiation as per manufacturer's instructions to demonstrate clinical translatability of our cell tracking approach. Chondrogenic differentiation was carried out by the pellet culture method in which 10^6 MSC were pelleted and cultured at 37°C and 5% CO₂ for 28 days with a complete media change every 3 days. Staining for murine and human MSCs was performed using Alcian Blue 8GX (Sigma) for chondrogenesis and Alizarin Red S (Sigma) for osteogenesis.

Gene expression

Murine MSCs were stimulated with 30 ng/mL murine interferon-gamma (Peprotech) at 37°C, 5% CO₂ for 18–20 hours. Post-stimulation, total RNA was isolated using TRIzol® Reagent (Life Technologies) and converted into cDNA with High-Capacity cDNA RT Kit (Life Technologies). Real-time RT PCR was performed using FastStart Universal SYBR Green Master mix (Roche). Samples were analyzed in triplicate for Beta2-Microglobulin (B2M), inducible NO synthase (iNOS), Interleukin 10 (IL10), Transforming growth factor beta (TGFβ1), Interleukin 6 (IL6), Hepatocyte growth factor (HGF), Programmed death-ligand 1 (PDL-1 or CD74) and Cyclooxygenase 2 (COX2 or Prostaglandin endoperoxide synthase 2, PTGS2) (see [S1 Table](#) for detailed primer sequences). Thermal cycling was performed with QuantStudio5 (ThermoFisher): 95°C, 2 min followed by 40 cycles of 95°C, 15s and 60°C, 20s. Relative fold change in expression levels were calculated using the 2^{-ΔΔCt} method, with Beta2-Microglobulin (B2M) as housekeeping gene [17]. Comparison was determined using paired Student's t-test.

Safety analysis

At 2 or 4 weeks after MSC or saline injections, whole blood, serum and heart and spleen tissues for histopathological analysis were collected from DMM and sham mice. Whole blood was collected by cardiac puncture immediately following sacrifice. For complete blood count (CBC) assessment, 100 μL of blood was collected per animal by capillary action into a Microvette® tube (Sarstedt) and stored at 4°C until analysis. To isolate serum, 200 μL of blood was collected by capillary action into a Microvette® tube with serum activators and allowed to clot for 60 minutes. Samples were then centrifuged at 10,000 g for 5 minutes at 4°C and serum was collected into a sterile microcentrifuge tube. Isolated serum was stored at -20°C until analysis at the Animal Resources Centres of the University Health Network. For histopathological assessment, heart and spleen were collected and fixed in 10% formalin, paraffin embedded, sectioned and stained with standard H&E for gross permit histopathological assessment by trained pathologist at the Pathology Core at The Centre for Phenogenomics.

Histopathology and image analysis

After the final MRI scanning session (at 1, 2 or 4 weeks after MSC or saline injections), mice were sacrificed and knee joints were isolated, fixed in 10% formalin. Mouse joints were decalcified using RDO Rapid Decalcifier (Apex Engineering). Cross sections of 4 mm of the medial aspect of the knee joints were deparaffinized, rehydrated and then underwent either histological or immunohistochemical staining.

Medial knee histological sections were stained with Safranin O dye to assess cartilage degradation and joint inflammation according to the OARSI (Osteoarthritis Research Society International) scoring system by Glasson et al. [18]. Briefly, rehydrated sections were stained with Weigert's Hematoxylin A and B (ThermoFisher Scientific, 50-317-75 and 50-317-79

respectively, 4 minutes), 0.01% Fast Green (Sigma Aldrich, F7252, 5 minutes), and 0.1% Safranin O (Sigma-Aldrich, S2255, 5 minutes). Sections were then dehydrated and mounted in Permount and imaged at 4x using a brightfield microscope. Synovial inflammation was determined according to OARSI histopathology methods [19]. Briefly, synovial inflammation is graded from 0–4, where 0 denotes no changes to synovial tissue, and 1–4 denotes the spectrum of synovial inflammation that includes: increased proliferation of subsynovial tissue, increased number of lining cell layers, and an increase in infiltration of inflammatory cells.

To evaluate fibrosis in the synovium, medial knee histological sections were stained with Masson's trichrome stain (Electron Microscopy Science #26367) according to the manufacturer's instruction. The sections scored for fibrosis on a scale of 0–3 (0, no fibrosis; 1, mild fibrosis; 2, moderate fibrosis; and 3, severe fibrosis [20]).

Immunohistochemistry and image analysis

Rehydrated sections that were to undergo immunohistochemical staining were first treated with 3% hydrogen peroxide to quench endogenous tissue peroxidases. Sections were then treated with Proteinase K (20 µg/mL) for 15 minutes for antigen retrieval and blocked with DAKO background reducing protein blocking agent (Agilent, X090930-2) prior to 1 hour incubation of anti-CD206 antibody (1:200, R&D systems, AF2535, S2 Table), anti-F4/80 antibody (1:100, Serotec, S2 Table), anti-iNOS antibody (1:100, Abcam, ab15323), Prussian Blue (equal volumes of 20% HCl in dH2O and 10% $K_4Fe(CN)_6 \cdot 3H_2O$ mixture, Sigma Aldrich respectively) and anti-Sca-1 antibody (1:100, Bio-Rad, MCA2782, S2 Table) at room temperature to detect homeostatic macrophages, total macrophages, proinflammatory macrophages, ferumoxytol-labeled MSCs and total cells respectively. Detection was performed using anti-goat secondary antibody (for CD206, 1:1000 Novus Biologicals, NB120-7124, S2 Table), anti-rat secondary antibody (for F4/80 and Sca-1, 1:500 Novus Biologicals, NBPI-75379, S2 Table) or biotinylated anti-rabbit secondary antibody (for cleaved caspase-3, 1:2000 or for iNOS, 1:200, Vector Labs BA-1000, S2 Table) for 30 minutes, followed by avidin-biotin complex detection system (VECTASTAIN Elite ABC system, Vector Labs PK-6100) for 30 minutes and DAB-horseradish peroxidase substrate detection system. Cells were counterstained with hematoxylin (Vector Labs, H3404) to detect total cells. Sections were subsequently dehydrated and mounted with Permount (ThermoFisher Scientific, SP15-500). Negative control staining was conducted by primary antibody exclusion for all markers. Hypertrophic chondrocytes within the growth plate was used as a positive control for caspase-3 (S1 Fig). Images were taken at 40x and analyzed with Fiji ImageJ software.

In analyzing macrophage populations, no difference was detected between DiR+MSCs and DiR+Fe-MSc treatment groups. Thus, quantification of CD206 positive macrophage populations was done by analytically pooling DiR+Fe-MScs and DiR MScs treatment groups in the DMM surgery groups, while only DiR+Fe-MScs was used in the SHAM-operated joints. This approach was not taken for iNOS positive macrophages, as this assay was done subsequently with a limited number of animals remaining.

Percentage of positively stained CD206 (homeostatic, "M2-like" cells) or iNOS (pro-inflammatory "M1-like" cells) or F4/80 (total macrophages) with respect to total cells (stained with Hematoxylin) was quantified. Then we calculated the ratio of cell proportions, namely % CD206: %F4/80 for homeostatic macrophages and %iNOS: %F4/80 for proinflammatory macrophages to assess synovial inflammation within the DMM or SHAM-operated knee joints. Briefly, 6–8 images were taken of medial knee joint sections at 40x to encompass the synovial tissue adjacent to the medial meniscus. Fiji (ImageJ) software was used to analyze the images. Specifically, each image underwent Colour Deconvolution to separate brown (DAB) channels

and purple (hematoxylin) channels. Subsequent images underwent “Threshold” such that positively stained cells were labeled as black. Positive cells were then quantified using the “Analyze Particles” feature with the following specifications: Size (pixel²):100–3000 and Circularity (0–0.8), which allowed for the software to provide a cell count for the respective stain. (This semi-automatic method of quantification was verified by doing manual counts of 20 images, which resulted in less than 15% error.) For statistical analysis, mean values were averaged to generate one value per individual per timepoint and the resulting average values were compared for statistical significance.

Results

Viability and phenotypic assessment of ferumoxytol-labeled MSC

Isolated murine MSC were characterized and shown to express SCA-1, CD90 and CD105 as well as iNOS and PDL-1, markers confirming mesenchymal stromal cells identity (S2 Fig). Analysis also indicated that the isolated cells were not hematopoietic or monocytic in origin as they showed CD45 levels ranging from 0.35% to 0.45% and CD11b levels ranging from 1.99% to 4.58% positive. This murine study serves as a precursor to human trials using ferumoxytol-labeled human MSCs, intra-articularly injected into patients with knee osteoarthritis and thus viability and differentiation was assessed for both murine and human MSCs. There were no differences osteogenic or chondrogenic differentiation potential of murine or human MSCs labeled with or without ferumoxytol (S3 Fig). Adipogenic differentiation was somewhat variable with murine MSCs and thus not reported. Similarly, trypan blue exclusion assay results demonstrated no difference in the viability of unlabeled and ferumoxytol-labeled-murine or human MSCs (with unlabeled and ferumoxytol (Fe)- murine MSCs demonstrating 98.5±1.9% and 94.3±5.9% viability, respectively S3 Fig).

Magnetic resonance imaging

Three-dimensional whole-body anatomical images were acquired that allowed well-defined delineation of experimental mouse knees over time. Representative images of control, sham and DMM surgical knees can be seen in Fig 2A. In control mouse knees a hyperintense region corresponding to the fat pad of the tibio-femoral joint was clearly evident (Fig 2A, red arrows). Both sham and DMM surgeries required the dissection of this fatpad to enable access to the joint and the absence of the fatpad was evident in all imaged sham and DMM surgical knees. Mice were imaged on the same day as, at three days post and either 1, 2 or 4 weeks post intra-articular saline or cell delivery. For sham and DMM surgery mice that received ferumoxytol labeled-MSC, MR images confirmed the intra-articular localization of the cells by the presence of distinct signal voids in the joint space (Fig 2A, red arrows). These signal voids were analyzed for void volume and fractional signal loss over time (Fig 2B and 2C). No external or MRI evidence of haemorrhage was observed in our saline control injected DMM and sham mice.

On the day of cell injection, the average volume of the region of signal loss within the surgical knee did not differ significantly between mice with different surgical preparations with a volume of 0.51±0.38 mm³ in DMM mice and 0.39±0.25 mm³ in sham mice (Fig 2A). In all DiR+Fe-MSC injected knees the void volume decreased overtime, however, a region of signal loss persisted in all knees at the transplant site until end point. A significantly greater percentage of the initial void volume persisted at 3 days and 1-week post DiR+Fe-MSC cell injection in DMM knees compared to sham knees (Fig 2B). By the 4-week end point both surgical groups showed a significant ($p < 0.0001$) reduction in void volume, but DMM surgery mice still retained a void volume of 0.17±0.04 mm³ which was significantly greater ($p = 0.001$) volume than the 0.06±0.03 mm³ void volume seen in sham surgery mice (Fig 2A). This difference

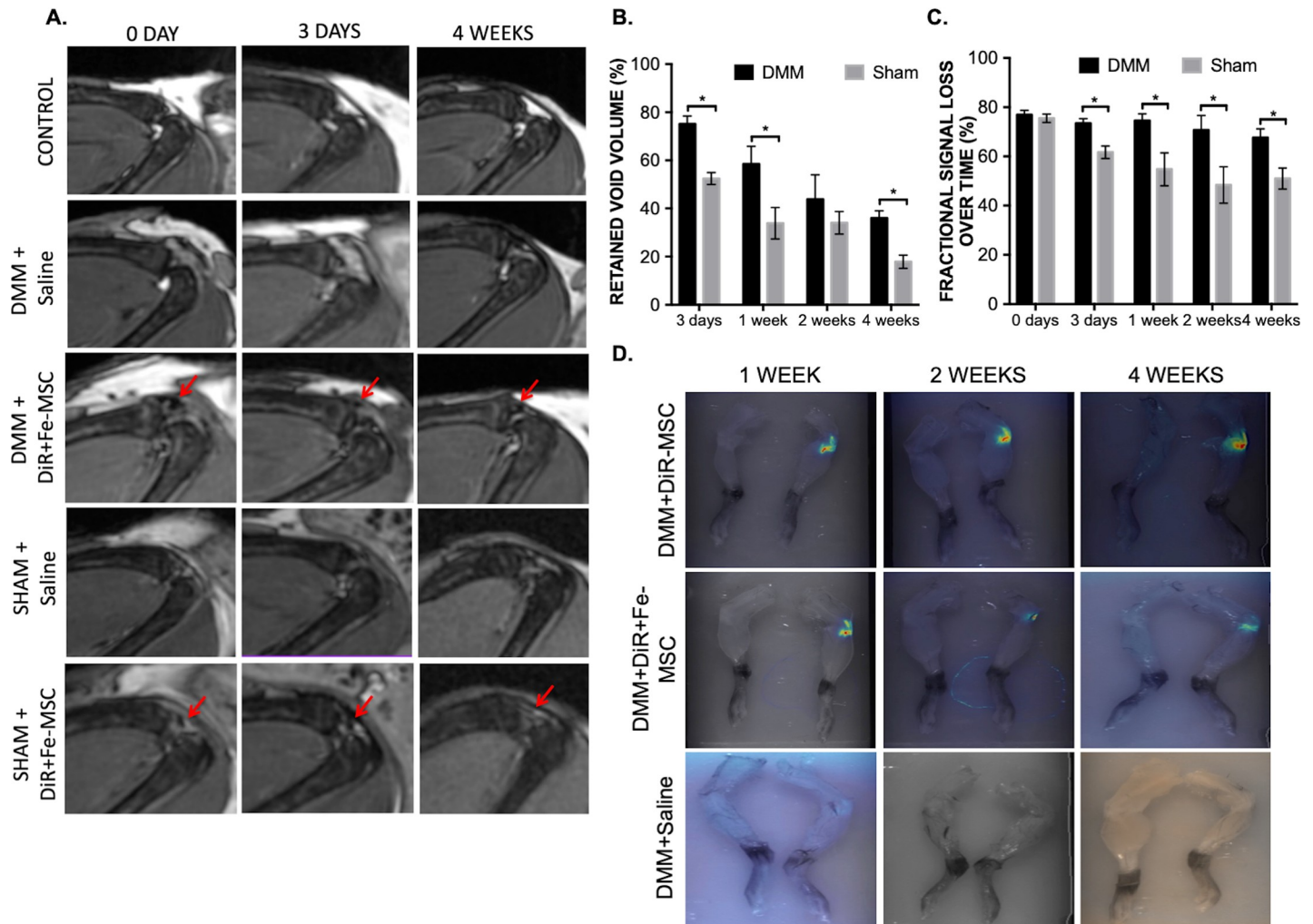


Fig 2. Persistence of MSCs in knee joints up to 4 weeks. (A) All mice received DMM or sham surgery 3 weeks prior to injection with either saline or 5×10^4 DiR +ferumoxylol-labeled MSCs (DiR+Fe-MSCs) or only DiR-labeled MSCs (DiR MSCs). Mice were imaged at day 0, 3 and at 4 weeks post intra-articular cell injection. Red arrows indicate the site of MSC implantation. Rows of images correspond to the same mouse over time. Control is contralateral knee without surgery or any manipulation of any kind. (B) Percent of retained void volume compared to day 0, showing MSCs presence in DMM and SHAM operated knee joints up to 4 weeks post-injection via MRI imaging (all ferumoxylol-labeled or unlabeled cells are DiR labeled). (C) Percent fractional signal loss (i.e. the difference in signal in the void divided by the signal in the surrounding tissue times 100) over time. * $p < 0.05$ between DMM and sham animals at the same time point as determined by Student's t-test and Tukey post-hoc test. (D) Persistence of MSCs in mouse joints over a period of 4 weeks, as displayed by DiR fluorescence labeling on all injected MSCs. Mice subjected to DMM+Saline was used as an imaging control.

<https://doi.org/10.1371/journal.pone.0214107.g002>

in void volume over time likely reflects a difference in the clearance of MSC and their associated iron oxide nanoparticles in DMM knees relative to sham surgery knees.

On the day of cell transplantation, the fractional signal loss (FSL) in DiR+Fe-MSC injected surgical knees did not differ significantly with FSL values of 77.0 ± 6.9 and 75.7 ± 6.3 for DMM and sham knees, respectively (Fig 2C). DMM surgery mice receiving DiR+Fe-MSC did not show a significant reduction in FSL over the time course of the experiment (Fig 2C). Conversely, sham surgery mice showed a significant ($p = 0.0021$) 18% reduction in FSL as early as 3 days post injection. The FSL observed in DMM versus sham surgery mice was significantly different ($p \leq 0.05$) at all assessed time points after the day of injection (Fig 2C). By the 4-week end point DiR+Fe-MSC injected DMM and sham surgery knees showed FSL values of 67.6 ± 8.0 and 51.0 ± 9.5 , respectively.

On the final day of imaging (at 1, 2 or 4 weeks) both the surgical and contralateral knees were collected and assessed for MSC persistence by fluorescent imaging. DiR fluorescence was detectable in DiR MSC and DiR+Fe-MS-C injected DMM surgical knees (Fig 2D). No fluorescence was evident in un-injected contralateral knees nor those injected solely with saline.

In addition to tracking DiR+Fe-MS-C implanted cells, longitudinal MRI analysis allowed the evaluation of suspected inflammation in the form of hyperintense fluid accumulation in surgical knees over time. DMM surgical knees receiving either vehicle (saline) or DiR+Fe-MS-C were scored with values between 1 and 5 where 1 represented no evidence of inflammation (no abnormal hyperintense signal visible) and 5 represented severe evidence of inflammation with very evident abnormal hyperintense signal and swelling beyond the normal joint space. On the day of cell implantation, the majority of DMM surgical knees showed evidence of inflammation; scores of 4.4 ± 0.7 and 4.0 ± 1.0 were recorded for saline and DiR+Fe-MS-C injected DMM knees, respectively (Fig 3A). At the 4-week end point DiR+Fe-MS-C injected DMM knees showed significantly less ($p = 0.01$) evidence of inflammation and were scored 1.2 ± 0.4 compared to saline knees scoring 3.6 ± 1.1 .

Retention of iron signal in MSCs

Histological sections were stained against Prussian Blue to further confirm presence of ferumoxytol in exogenously injected MSCs [21]. As there was no specific marker that could be used to distinguish between the syngeneic murine MSCs injected and the endogenous MSCs present, we relied on Prussian Blue staining to indicate the persistence of the injected MSC. There has been no reported incidence of phagocytic activity from endogenous MSCs or hematopoietic stem cells, and thus we did not expect ferumoxytol from injected MSCs to be found within any endogenous cells, MSCs or hematopoietic stem cells. Therefore, Sca-1+ and Prussian Blue double positive (ferumoxytol) cells (in Fig 4A) would indicate injected exogenous MSCs, while Sca-1 positive but Prussian Blue negative cells would indicate endogenous MSCs and/or hematopoietic cells. Prussian Blue staining was found to localize within the synovial joint, indicating that ferumoxytol-labeled MSCs do persist in the joint space up to 4 weeks after intra-articular injection. Notably, positively stained Prussian Blue labeled MSCs (blue) were detected within macrophages (stained with F4/80, purple) as early as 1 week after intra-articular injection, suggesting that macrophages engulfed apoptotic MSC bodies during the early inflammatory phase of osteoarthritis (Fig 4B). This is confirmed by presence of cleaved Caspase-3 positive, Sca-1 and Prussian Blue positive cells suggesting apoptotic MSCs that were exogenously introduced as they contain the iron nanoparticles.

Histopathology of Synovial Joints

Cartilage degeneration of mouse joints was graded using the OARSI scoring system. No significant changes were found in cartilage degradation or synovitis between MSC-treated and saline-treated OA-mice. (Fig 3B).

Using the OARSI scoring system for synovial inflammation [19], average synovial inflammation scores (0–4) were determined in DMM-operated mice treated with saline or DiR+Fe-MS-Cs. Differences in hyperintense signal, reflective of fluid edema in the joint were detected via MR imaging during the early phase of inflammation (i.e. 3 days) and late inflammation (i.e. 4 weeks) after MSC treatment ($p < 0.05$ respectively).

The substantial decrease in knee-associated edema at 4 weeks after MSC injection (Fig 3A) corresponded with the prolonged persistence of DiR+Fe-MS-Cs within the synovial joint (Fig 2), and an increase of homeostatic macrophages at 4 weeks after injection (Fig 5), suggesting that the MSC treatment may be contributing significantly to the infiltration and polarization

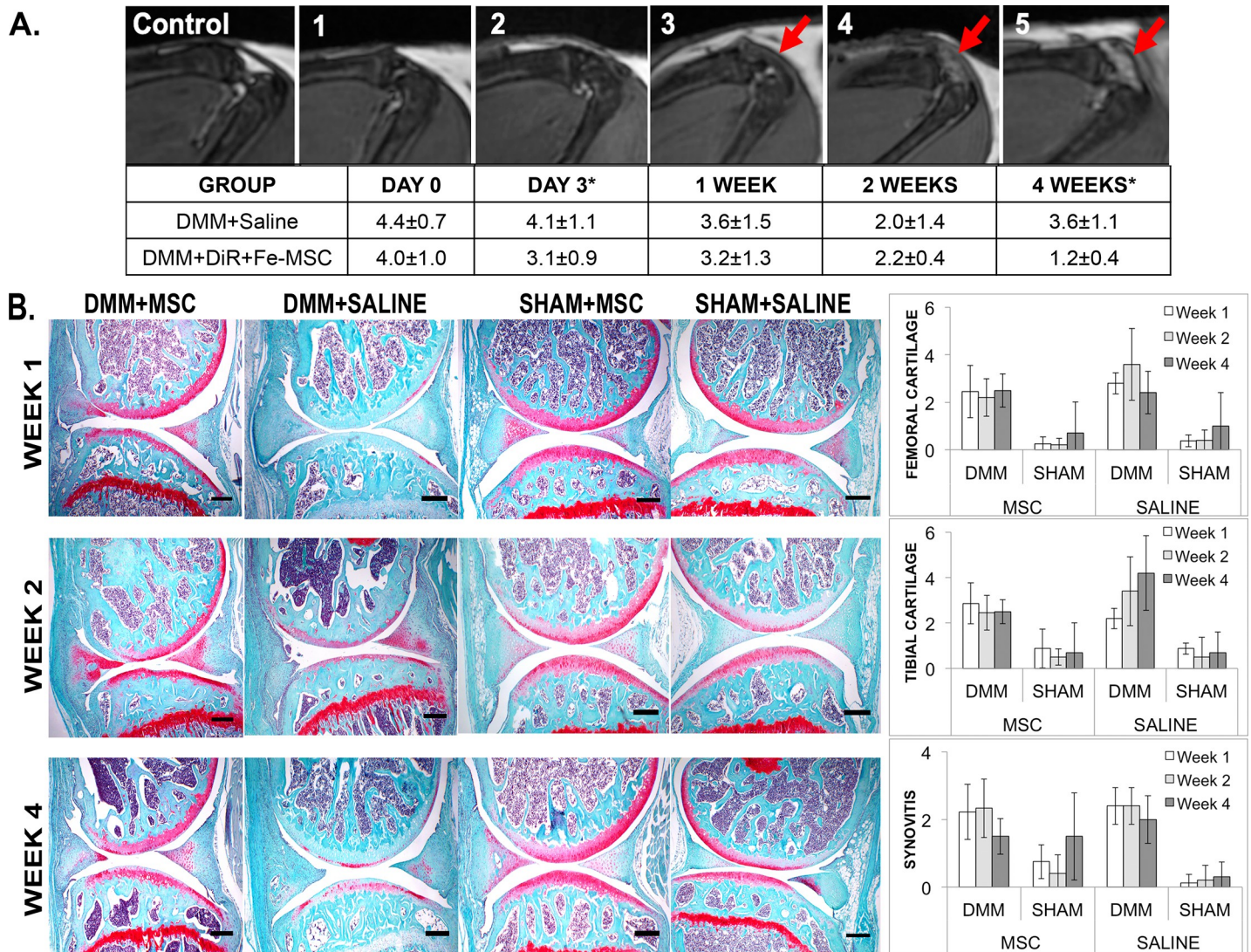


Fig 3. Joint Inflammation, cartilage degradation and synovitis assessments on DMM or SHAM-operated joints treated with MSCs. (A) MRI assessment of joint inflammation with representative images to indicate scale. The following scale corresponds to amount of swelling observed in the joint. 1 = Not evident; 2 = Unlikely; 3 = Uncertain; 4 = Likely; 5 = Clear Evidence. The table indicates representative joint inflammation scores on DMM-operated mice treated with or without DiR+Fe-MSC. Significance was found at Day 3 and Week 4 mouse groups (* $p < 0.05$). These images are representative of both DiR+Fe-MSCs and DiR MSCs. Arrows indicate the site of abnormal hyperintense signal detected in the mouse knee. (B) OARSIS scoring for of DMM-operated or SHAM-operated joints treated with MSC or saline were assessed on Safranin O-stained sections. No significant difference in cartilage degradation or synovitis was observed between all groups. The OARSIS scores were calculated by including the scores of both DiR+Fe-MSCs and DiR MSCs injection in the DMM surgery groups while only DiR+Fe-MSCs was used in the SHAM-operated joints. Scalebar = 500 μ m).

<https://doi.org/10.1371/journal.pone.0214107.g003>

of macrophages into a more homeostatic phenotype to resolve synovial inflammation within the joint.

Immunohistochemistry

In analyzing macrophage populations, no difference was detected between DiR+MSCs and DiR+Fe-MSC treatment groups. Thus, quantification of CD206 positive macrophage populations was done by analytically pooling both MSCs treatment groups that received DMM surgery and comparing those to saline only treated knees. As this study was primarily focused on

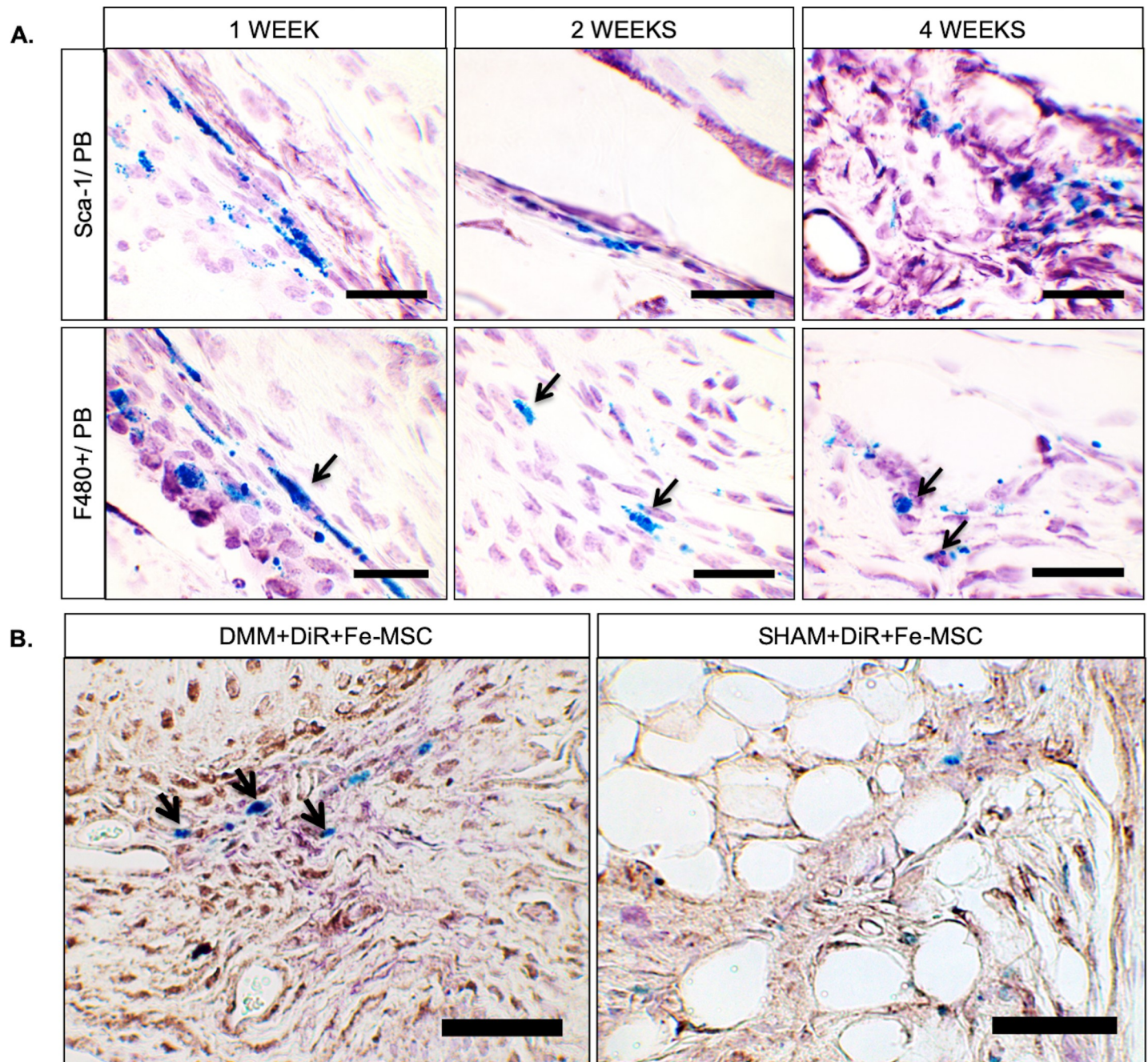


Fig 4. Histopathological analyses of MSCs in DMM-operated mice at 1, 2, and 4 weeks post-injection. (A) Mouse knee sections were co-stained with Sca-1 (Purple) and Prussian Blue (PB, blue) to indicate persistence of DiR+Fe-MSc at 1, 2 and 4 weeks post-injection. Co-staining of F4/80 (purple) and Prussian Blue (blue) demonstrated some co-localization of DiR+Fe-MSc cells with macrophages. (Black Arrows.) Scalebar = 50 μ m. (B) Mouse knee sections were triple-labeled with Sca-1 (Purple), cleaved Caspase-3 (brown), and Prussian Blue (blue), to indicate presence of apoptotic DiR+Fe-MSCs in synovium. Scalebar = 50 μ m.

<https://doi.org/10.1371/journal.pone.0214107.g004>

the feasibility of tracking Fe-labeled MSCs in a clinically relevant OA animal model we did not specifically analyze any immunomodulatory profile differences between Fe-labeled and unlabeled MSC. As a means to examine the possible mechanism of action for MSC treatments in an OA joint in general, medial knee sections were stained against CD206, F4/80 and subsequently with iNOS and Masson's Trichrome to determine the changes in the types of

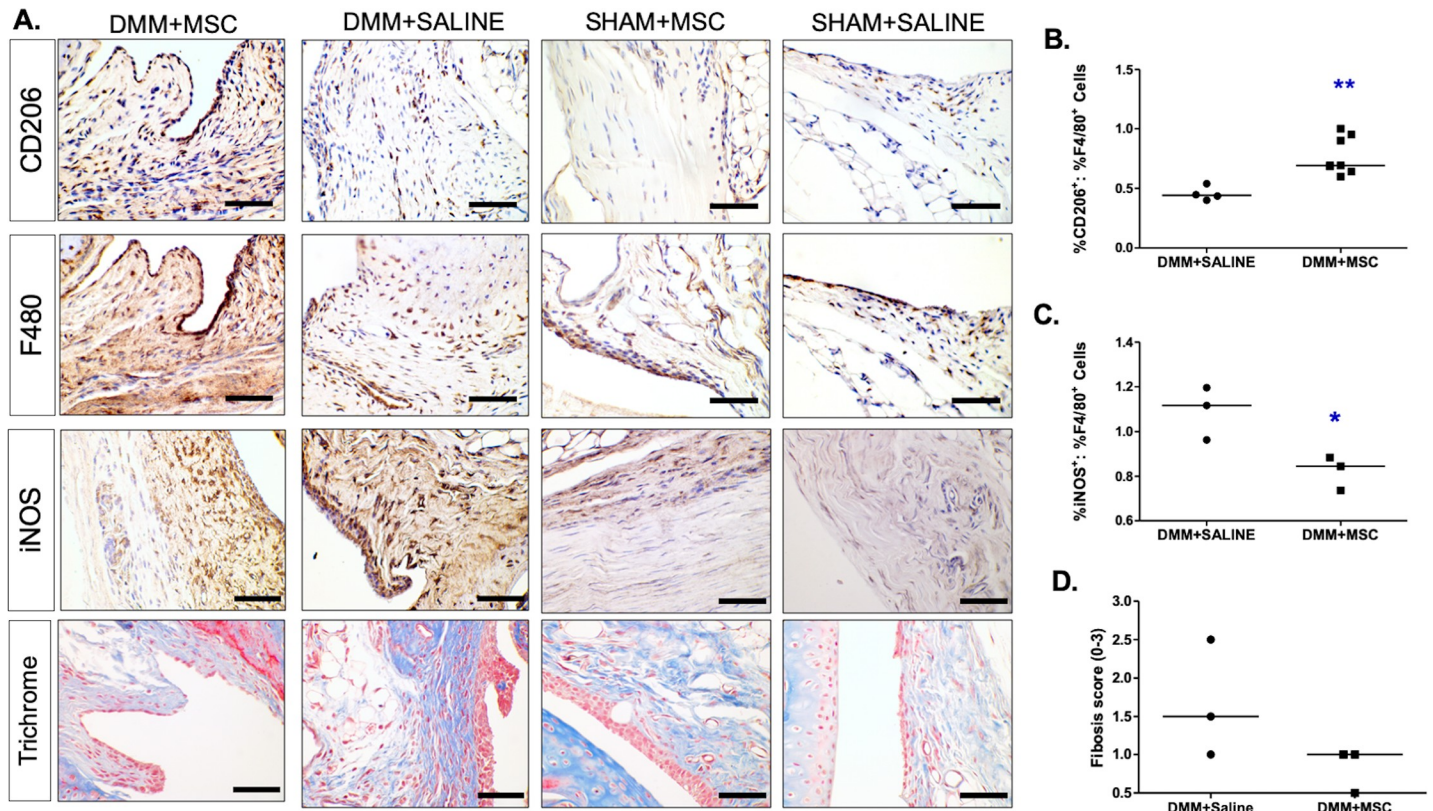


Fig 5. MSC treatment promoted an increase in homeostatic macrophage- (CD206⁺) and a decrease in pro-inflammatory cells (iNOS⁺), and reduced fibrosis in osteoarthritic synovium at 4 weeks post-treatment. (A) Sections from DMM-operated and SHAM-operated mice treated with MSC or saline were stained with CD206 (brown, n = 7), iNOS (brown, n = 3), F4/80 (brown, n = 7) and hematoxylin (blue, n = 7) to detect homeostatic macrophages, proinflammatory macrophages, total macrophages and total cells respectively (Scale bar = 50 μ m). The last row of images shows Masson's trichrome staining of sections representing fibrosis (n = 3). (B and C) Quantification of ratio of positively stained %CD206⁺:%F4/80⁺ cells (n = 7 animals) and positively stained %iNOS⁺:%F4/80⁺ cells (n = 3 animals), respectively. DMM-operated mice treated with MSC yielded significantly more CD206⁺ cells (homeostatic macrophage) relative to the proportion of F4/80 positive macrophages (**p<0.01, one data point from DMM+SALINE group was a significant outlier and excluded from analysis) and significantly lower iNOS positive cells (*p<0.05) in the synovium than vehicle treated OA mice. (D) Grading of sections stained Masson's trichrome on a scale of 0–3 (0, no fibrosis; 1, mild fibrosis; 2, moderate fibrosis; and 3, severe fibrosis).

<https://doi.org/10.1371/journal.pone.0214107.g005>

macrophages, and to assess fibrosis in the joint MSC injection in OA-induced mice (Fig 5A). Specifically, we also quantified the ratio of the signals to assess changes in macrophage subtypes. There was a significant increase in the ratio of %CD206⁺:%F4/80⁺ macrophages (p<0.01, Fig 5B) and a significant reduction in the ratio of %iNOS⁺:%F4/80⁺ macrophages (p<0.05, Fig 5C), suggesting an increase in inflammation-resolving homeostatic macrophages and a reduction in pro-inflammatory cells. There was also a trend (non-significant) towards reduction in the fibrosis scores in mice receiving MSCs, suggesting that MSC treatment led to an increase in macrophage polarization towards a homeostatic phenotype (p<0.01, Fig 5B and 5C), and to reduced fibrosis (p = 0.158, Fig 5D).

Safety of ferumoxytol-labeled MSCs vs. unlabeled MSCs

Safety of ferumoxytol-labeled MSC over a 4-week period was also verified in 35 mice with histology on target organs, and CBC and blood biochemistry (S3 and S4 Tables). Our data shows no difference in read-outs between ferumoxytol-labeled and unlabeled MSCs, saline controls or sham animals.

Discussion

Using a non-invasive clinically-approved tracking method, we have for the first time imaged ferumoxytol-labeled MSC persistence in an *immunocompetent clinically translatable* mouse model of surgically-induced osteoarthritis (OA). We showed persistence of MSCs out to four weeks after injection, and importantly suggested a potential anti-inflammatory mechanism of actions involving MSCs polarization of joint-specific macrophages to more homeostatic lineages.

Previously, serial scans of xenotransplanted human MSCs (hMSCs) in an osteochondral rat defect model showed that the iron signal of apoptotic, nanoparticle-labeled hMSCs engulfed by macrophages disappeared faster compared to viable hMSCs in T2-weighted MRI images [22]. This corresponded to poor cartilage repair outcomes in rats receiving apoptotic hMSCs.

Delling et al. similarly used a non-vital ovine MSC group in 12 sheep that had OA-induced by bilateral meniscectomy and reported significant differences in hypointensity signaling up to 12 weeks between the vital and non-vital MSC groups [23]. Importantly, they observed reduced Prussian Blue staining in sheep receiving the non-vital MSCs by immunohistology compared to vital MSC groups. They did report increased chondrogenic differentiation surrounding regions of iron nanoparticle detection.

We report for the first time, that Prussian Blue staining by immunohistochemistry is largely visible in cells that co-stain for Sca-1, a marker of bone marrow-derived mesenchymal stromal cells [24]. Interestingly, we also show Prussian Blue co-staining with F4/80 positive cells, suggestive of iron nanoparticle signal uptake by macrophages in the joint. This likely suggests phagocytosis of apoptotic MSCs by joint macrophages as evidenced by our data showing cleaved Caspase 3 positive, Sca-1 positive, Prussian Blue positive cells (Fig 4). However, unlike Daldrup et al., we do not see a diminishment in repair properties due to apoptotic MSCs. In fact, the DMM mice showed the same degree of cartilage degradation with or without MSC injection, 4 weeks post-MSc injection. Recently exosomes from pluripotent stem cell-derived MSCs were reported to improve cartilage degradation in a DMM model [25]. However, the authors used repeated MSC exosome injections (every 3 days over a 4-week period) to achieve this effect. Here, we used a single MSC injection, which also decreased the amount of injury to the synovial joint upon delivery of treatment. In addition, there were xeno- and tissue-source differences: Wang et al. used human embryonic stem cell-derived MSCs while we used murine femur-derived MSCs [25].

In fact, we showed that despite the potential apoptosis of MSCs, there was an increased skewing of macrophages to more homeostatic lineages, based on expression of CD206, relative to mice receiving placebo controls. CD206 is a classical marker of more homeostatic macrophages, as a mannose receptor involved in phagocytosis [26–28]. Recently it has been suggested that apoptosis of MSCs may in fact enhance their immunosuppressive properties, eliciting an IL10, IDO and TGFβ1 suppressive response similar to efferocytosis of apoptotic cell debris [29,30] as we have observed.

Macrophages are key mediatory cells of synovial inflammation and fibrosis or synovitis, a hallmark characteristic of OA pathology [31]. We have recently shown that prevalence of pro-inflammatory monocytes/macrophages in knee OA patients inversely correlates to worsening patient-reported outcomes [15]. Others have similarly reported that prevalence of folate-receptor (i.e., activated) macrophages correlates with OA severity [31]. Pro-inflammatory monocytes/macrophages produce inflammatory and degradatory mediators [32], activate T cells and the complement system [32], and inhibit chondrogenesis in vitro [33]. Notably, we reported a decrease in pro-inflammatory monocytes/macrophages after MSC injection in our MSC OA clinical trial [8]. We noted a decrease in the proportion of iNOS positive cells relative

to the proportion of macrophages, but note that this marker is not specific to pro-inflammatory macrophages and is present on multiple cell types in the joint. Nonetheless, expression of this pro-inflammatory marker decreases with MSC injection [31–33].

Others have also previously reported that MSC injection into DMM models does not result in improvement to cartilage scores, consistent with our results in this study, and indeed with our clinical observations in a 12 patient MSC knee OA trial [8]. Schelbergen et al. have previously shown that adipose tissue-derived (AT) MSCs improved synovitis outcomes, which are pronounced in a collagenase-induced OA (CIOA) model, but not in a DMM model [34]. Unlike this study, which primarily reported AT-MS-mediated reduced synovitis in the CIOA, we did investigate changes to inflammation even in this mild-inflammatory model, and report that MSC treatment does reduce synovial inflammation and fibrosis.

There is a need to specifically track MSCs following clinical infusion to evaluate their migration within the arthritis joint, and to quantify their accumulation and short-term persistence at the target, and elsewhere in the body. This in turn will enable better dosing and design of Phase II clinical investigations. Our findings show feasibility of using ferumoxytol (Feraheme™) for tracking short-term persistence and biodistribution of MSCs. Ferumoxytol as an iron replacement product indicated for the treatment of iron deficiency anemia in adult patients with chronic kidney disease (CKD) (DIN # 02377217). Importantly, we showed no differences in murine and human (S2 Fig) MSCs in terms of their viability, cell surface markers or tri-lineage differentiation capacity. Ferumoxytol-labeled MSCs were similar to unlabeled MSCs in terms of blood chemistry and gross histopathology of target organs (heart and spleen) (S2 and S3 Tables). This is important to note as some adverse findings have been reported with intravenous use of ferumoxytol at doses that are 600-fold higher than what we propose for ex-vivo labeling of MSCs (only 10% of MSCs will be labeled in a clinical infusion scenario). Recently, off-label use of ferumoxytol as a contrast agent (single 5 mg/kg or 4x doses) in 49 pediatric patients and 19 adults showed no serious adverse events and 4 mild, self-resolving adverse events [35]. This dose is 6.67-fold greater than the 0.75 mg dose we are proposing. Three investigation new drug applications (IND) (NCT02006108, NCT01336803 and NCT02893293) using ferumoxytol as a contrast agent were approved by the FDA; one clinical trial application (CTA, NCT02466828) using ferumoxytol as a contrast agent was approved by Health Canada. These proposed doses are 120-fold lower than the approved intra-venous dose, and about 6.67-fold higher than what we would propose to use in a clinical tracking study of MSCs. In this trial, we plan to inject up to 10% ferumoxytol-labeled MSCs of the total dose (10% labeled MSCs + 90% unlabeled MSCs) and track them at different time points by MRI imaging. Our findings lay the ground work for a clinical pharmacokinetics/pharmacodynamics study of MSCs in osteoarthritis. Our findings confirm an anti-inflammatory mechanism of action of MSCs in osteoarthritis.

Our study represents a valuable step in the evaluation of ferumoxytol-based cell tracking and serves as a prelude to human trials using ferumoxytol-labeled human MSCs in patients with knee osteoarthritis. There were several limitations to our study. First, our use of a syngeneic animal model limited our ability to differentiate injected MSC from any endogenous MSC present within the knee. We believe that our ability to perform our assessments in the presence of an intact immune system using this model outweighed this limitation. Also, most preclinical imaging is conducted at higher field strengths to obtain optimal image resolution of small structures, however, we routinely and intentionally performed our cell tracking studies at field strengths within the realm of clinical imaging in aims of translating our approach towards a clinical investigation. Clinical imaging typically utilizes a local knee coil for knee imaging, however, for our study we performed whole body imaging. This choice was made based on our available imaging hardware and despite this limitation we successfully achieved

200 μm resolution of the mouse knee. While iron oxide is a popular contrast agent choice for MRI cell tracking due to its improved sensitivity over other MRI contrast agents [36], we recognize that it can also cause signal voids that can be confused with air or other iron sources such as in an hemorrhage. In our study, particular care was taken to avoid the introduction of air at the injection site and no evidence of hemorrhage was observed at the time of DMM surgery. We recognize that hemorrhage did have the potential to form in our animal model over the course of the experiment, however, discernable signal voids were evident at the site of injection solely in ferumoxytol-labeled MSC injected surgical knees and were found to persist at the detected injection site over time. This was not observed in control animals including those in which saline was injected into the surgical knee. Some of our findings may have been strengthened by increased sample number, which was limited by the cost of conducting extensive MR imaging. Our sample number, however, permitted the successful demonstration of ferumoxytol-labeled MSC persistence in a clinically translatable mouse model of OA for up to 4 weeks and provided sufficient data to illustrate a potential mechanism of action involving MSCs polarization of joint-specific macrophages to more homeostatic lineages. Finally, we observed no changes in cartilage degradation in surgical knees over the course of our study and this was likely due to the timeline of our investigation. Typically, DMM treated mice are followed out to 8–16 weeks after DMM surgery when changes in cartilage degradation are observed [16]. These time points are too long for us to perform iron-based short-term cell tracking as ferumoxytol is a biodegradable nanoparticle that cannot be retained for such long durations [37]. might be to reduce synovial inflammation and fibrosis, and this was supported by our data, which showed an increase in inflammation-resolving macrophages in the synovium, and a decrease in pro-inflammatory cells, and decrease in fibrosis. The MSC effects on the synovium may translate into effects on the cartilage, but this would occur at later timepoints than set up in our study. For this study, our main focus was to evaluate the feasibility of iron-based short-term cell tracking for injection localization and initial tracking following cell administration and subsequently chose to limit imaging follow-up to 4 weeks post MSC injection.

Summary

We have shown that ferumoxytol-labeled murine MSCs can be tracked by MRI imaging in murine osteoarthritic joints without adverse events for up to 4 weeks. Ferumoxytol labeling of MSCs caused no alterations in viability, gene expression or osteogenic and chondrogenic differentiation potential. Ferumoxytol-labeled MSCs persisted for a longer periods of time in surgically-injured DMM mice joints than in SHAM controls. Persistence of the ferumoxytol label in MSCs was confirmed by double staining of Sca-1+ positive cells with Prussian Blue. The presence of Prussian Blue staining in neighboring macrophages argues for efferocytosis of apoptotic MSCs (additionally stained for Cleaved Caspase-3), which has recently been shown as a viable mechanism that enhances MSC immunomodulation. We report for the first time that DMM mice receiving MSCs had an increased proportion of homeostatic polarized macrophages, reduced pro-inflammatory macrophages and tendency to reduced fibrosis in the arthritic joint than control groups, suggesting that MSCs may have anti-inflammatory effects on OA synovitis. Taken together, our imaging study provides additional insights into MSC mechanism of action and lays the groundwork for short-term clinical tracking studies using ferumoxytol-labeled MSCs.

Supporting information

S1 Fig. Immunohistochemistry controls. (A) Controls for Rabbit-Anti-Mouse cleaved Caspase-3 antibody. (Left) Synovial tissue was stained with anti-rabbit secondary only,

counterstained with hematoxylin. (Right) Caspase-3 displayed specific immunostain in growth plate control, as hypertrophic chondrocytes undergo apoptosis within the growth plate. (B) No primary Antibody negative control for and iNOS (Top left) CD206 (Top right), F4/80 (Lower left) and Sca-1 (lower right) respectively, using anti-goat secondary and anti-rat secondary antibody. Scalebars are 100 μ m.

(TIFF)

S2 Fig. Mouse MSC characterization. (A) Immunophenotyping of murine MSCs. Blue histograms represent unstained cells and red overlay histograms are for positive MSC markers (Sca-1, CD90, CD105) and negative hematopoietic markers (CD45, CD11b, CD34). MSC associated (shown in red) and non-associated markers (shown in blue). Table (right) indicates the percent expression of each marker for both cell populations. (B) Differential gene expression analysis of MSC. Data shown are fold change relative to housekeeping gene mouse beta-2-microglobulin (mB2M) as analyzed by qPCR. (C) Osteogenic differentiation and chondrogenic differentiation of MSCs using Human Mesenchymal Stem Cell (hMSC) Differentiation Kit (ThermoFisher). Images were taken using EVOS microscope at 10X magnification (scale bar:100 μ m).

(TIFF)

S3 Fig. Analysis of differentiation potential, viability and gene expression of ferumoxytol-labeled and unlabeled murine and human MSCs. (A) Chondrogenesis stained with Alcian Blue and (B) Osteogenesis stained with Alizarin Red S. Scalebar = 25 μ m; mMSC: murine MSC; hMSC: human MSC. C. No viability differences in ferumoxytol-labeled murine and human MSCs vs. unlabeled murine and human MSCs. Viability assessed by Trypan Blue exclusion assay expressed as percentages. murine MSCs (n = 4). human MSCs (n = 3).

(TIFF)

S1 Table. Primer sequences used for the PCR.

(DOCX)

S2 Table. List of antibodies used in the MSC immunophenotypic characterization by flow cytometry and their clone numbers.

(DOCX)

S3 Table. Blood chemistry results in mice receiving DiR+FeMSCs vs. DiR MSCs at 2 and 4 weeks.

(DOCX)

S4 Table. Pathology report after injection of DiR+Fe-MSCs vs. DiR MSCs at 2 and 4 weeks. The report shows that Fe-MSCs are safe as assessed by gross pathology of heart and spleen. n/s: No significant findings; H*: The majority of the myocardium appears normal. There is one region of endocardium that has a small amount of fibrin deposition. Duration: subacute; Distribution: focal; Severity: moderate; S*: There are a few areas of decreased density in the periphery of the red pulp. The marginal zones also appear moderately decreased.

(DOCX)

Acknowledgments

The authors would like to acknowledge the Pathology Core at The Centre for Phenogenomics as well as the Animal Resources Centres of the University Health Network and of the University of Western Ontario for their technical services. We declare that there was no role of the

funding source on the design of the study and collection, analysis, and interpretation of data and in writing the manuscript.

Author Contributions

Conceptualization: Paula J. Foster, Sowmya Viswanathan.

Data curation: Paula J. Foster, Sowmya Viswanathan.

Formal analysis: Amanda M. Hamilton, Wing-Yee Cheung, Razieh Rabani.

Funding acquisition: Sowmya Viswanathan.

Investigation: Amanda M. Hamilton, Wing-Yee Cheung, Sowmya Viswanathan.

Methodology: Amanda M. Hamilton, Wing-Yee Cheung, Alejandro Gómez-Aristizábal, Anirudh Sharma, Sayaka Nakamura, Amélie Chaboureau, Shashank Bhatt, Razieh Rabani, Mohit Kapoor, Paula J. Foster, Sowmya Viswanathan.

Project administration: Amélie Chaboureau, Sowmya Viswanathan.

Resources: Amélie Chaboureau, Mohit Kapoor, Paula J. Foster, Sowmya Viswanathan.

Software: Paula J. Foster.

Supervision: Mohit Kapoor, Paula J. Foster, Sowmya Viswanathan.

Validation: Sowmya Viswanathan.

Visualization: Sowmya Viswanathan.

Writing – original draft: Amanda M. Hamilton, Wing-Yee Cheung, Sowmya Viswanathan.

Writing – review & editing: Amanda M. Hamilton, Wing-Yee Cheung, Alejandro Gómez-Aristizábal, Anirudh Sharma, Sayaka Nakamura, Amélie Chaboureau, Shashank Bhatt, Mohit Kapoor, Paula J. Foster, Sowmya Viswanathan.

References

1. Hootman JM, Helmick CG, Barbour KE, Theis KA, Boring MA (2016) Updated Projected Prevalence of Self-Reported Doctor-Diagnosed Arthritis and Arthritis-Attributable Activity Limitation Among US Adults, 2015–2040. *Arthritis Rheumatol* 68: 1582–1587. <https://doi.org/10.1002/art.39692> PMID: 27015600
2. Lamo-Espinosa JM, Mora G, Blanco JF, Granero-Molto F, Nunez-Cordoba JM, et al. (2016) Intra-articular injection of two different doses of autologous bone marrow mesenchymal stem cells versus hyaluronic acid in the treatment of knee osteoarthritis: multicenter randomized controlled clinical trial (phase I/II). *J Transl Med* 14: 246. <https://doi.org/10.1186/s12967-016-0998-2> PMID: 27565858
3. Pers YM, Rackwitz L, Ferreira R, Pullig O, Delfour C, et al. (2016) Adipose Mesenchymal Stromal Cell-Based Therapy for Severe Osteoarthritis of the Knee: A Phase I Dose-Escalation Trial. *Stem Cells Transl Med* 5: 847–856. <https://doi.org/10.5966/sctm.2015-0245> PMID: 27217345
4. Vega A, Martin-Ferrero MA, Del Canto F, Alberca M, Garcia V, et al. (2015) Treatment of Knee Osteoarthritis With Allogeneic Bone Marrow Mesenchymal Stem Cells: A Randomized Controlled Trial. *Transplantation* 99: 1681–1690. <https://doi.org/10.1097/TP.0000000000000678> PMID: 25822648
5. Orozco L, Munar A, Soler R, Alberca M, Soler F, et al. (2013) Treatment of knee osteoarthritis with autologous mesenchymal stem cells: a pilot study. *Transplantation* 95: 1535–1541. <https://doi.org/10.1097/TP.0b013e318291a2da> PMID: 23680930
6. Bastos R, Mathias M, Andrade R, Bastos R, Balduino A, et al. (2018) Intra-articular injections of expanded mesenchymal stem cells with and without addition of platelet-rich plasma are safe and effective for knee osteoarthritis. *Knee Surg Sports Traumatol Arthrosc* 26: 3342–3350. <https://doi.org/10.1007/s00167-018-4883-9> PMID: 29511819
7. Saw KY, Anz A, Siew-Yoke Jee C, Merican S, Ching-Soong Ng R, et al. (2013) Articular cartilage regeneration with autologous peripheral blood stem cells versus hyaluronic acid: a randomized controlled trial. *Arthroscopy* 29: 684–694. <https://doi.org/10.1016/j.arthro.2012.12.008> PMID: 23380230

8. Chahal J, Gomez-Aristizabal A, Shestopaloff K, Bhatt S, Chaboureaux A, et al. (2019) Bone Marrow Mesenchymal Stromal Cells in Patients with Osteoarthritis Results in Overall Improvement in Pain and Symptoms and Reduces Synovial Inflammation. *Stem Cells Transl Med*.
9. Laria A, Lurati A, Marrazza M, Mazzocchi D, Re KA, et al. (2016) The macrophages in rheumatic diseases. *Journal of Inflammation Research* 9: 1–11. <https://doi.org/10.2147/JIR.S82320> PMID: [26929657](https://pubmed.ncbi.nlm.nih.gov/26929657/)
10. O'Brien K, Tailor P, Leonard C, DiFrancesco LM, Hart DA, et al. (2017) Enumeration and Localization of Mesenchymal Progenitor Cells and Macrophages in Synovium from Normal Individuals and Patients with Pre-Osteoarthritis or Clinically Diagnosed Osteoarthritis. *International Journal of Molecular Sciences* 18: 774.
11. Thu MS, Bryant LH, Coppola T, Jordan EK, Budde MD, et al. (2012) Self-assembling nanocomplexes by combining ferumoxytol, heparin and protamine for cell tracking by magnetic resonance imaging. *Nat Med* 18: 463–467. <https://doi.org/10.1038/nm.2666> PMID: [22366951](https://pubmed.ncbi.nlm.nih.gov/22366951/)
12. Khurana A, Nejadnik H, Chapelin F, Lenkov O, Gawande R, et al. (2013) Ferumoxytol: a new, clinically applicable label for stem-cell tracking in arthritic joints with MRI. *Nanomedicine (Lond)* 8: 1969–1983.
13. Sato M, Uchida K, Nakajima H, Miyazaki T, Guerrero AR, et al. (2012) Direct transplantation of mesenchymal stem cells into the knee joints of Hartley strain guinea pigs with spontaneous osteoarthritis. *Arthritis Res Ther* 14: R31. <https://doi.org/10.1186/ar3735> PMID: [22314040](https://pubmed.ncbi.nlm.nih.gov/22314040/)
14. Toupet K, Maumus M, Peyrafitte JA, Bourin P, van Lent PL, et al. (2013) Long-term detection of human adipose-derived mesenchymal stem cells after intraarticular injection in SCID mice. *Arthritis Rheum* 65: 1786–1794. <https://doi.org/10.1002/art.37960> PMID: [23553439](https://pubmed.ncbi.nlm.nih.gov/23553439/)
15. Gómez-Aristizábal A GR, Marshall WK, Mahomed N, Viswanathan S. (2019) Synovial fluid levels of monocyte/macrophages and T cells correlates with osteoarthritis clinical and radiographic outcomes. *Arthritis Research & Therapy* 21(1): 26.
16. Glasson SS, Blanchet TJ, Morris EA (2007) The surgical destabilization of the medial meniscus (DMM) model of osteoarthritis in the 129/SvEv mouse. *Osteoarthritis Cartilage* 15: 1061–1069. <https://doi.org/10.1016/j.joca.2007.03.006> PMID: [17470400](https://pubmed.ncbi.nlm.nih.gov/17470400/)
17. Livak KJ, Schmittgen TD (2001) Analysis of relative gene expression data using real-time quantitative PCR and the 2^{(-Delta Delta C(T))} Method. *Methods* 25: 402–408. <https://doi.org/10.1006/meth.2001.1262> PMID: [11846609](https://pubmed.ncbi.nlm.nih.gov/11846609/)
18. Glasson SS, Chambers MG, Van Den Berg WB, Little CB (2010) The OARSI histopathology initiative—recommendations for histological assessments of osteoarthritis in the mouse. *Osteoarthritis Cartilage* 18 Suppl 3: S17–23.
19. Gerwin N, Bendele AM, Glasson S, Carlson CS (2010) The OARSI histopathology initiative—recommendations for histological assessments of osteoarthritis in the rat. *Osteoarthritis Cartilage* 18 Suppl 3: S24–34.
20. Krenn V, Morawietz L, Haupl T, Neidel J, Petersen I, et al. (2002) Grading of chronic synovitis—a histopathological grading system for molecular and diagnostic pathology. *Pathol Res Pract* 198: 317–325. <https://doi.org/10.1078/0344-0338-5710261> PMID: [12092767](https://pubmed.ncbi.nlm.nih.gov/12092767/)
21. Liu L, Tseng L, Ye Q, Wu YL, Bain DJ, et al. (2016) A New Method for Preparing Mesenchymal Stem Cells and Labeling with Ferumoxytol for Cell Tracking by MRI. *Sci Rep* 6: 26271. <https://doi.org/10.1038/srep26271> PMID: [27188664](https://pubmed.ncbi.nlm.nih.gov/27188664/)
22. Daldrup-Link HE, Golovko D, Ruffell B, Denardo DG, Castaneda R, et al. (2011) MRI of tumor-associated macrophages with clinically applicable iron oxide nanoparticles. *Clin Cancer Res* 17: 5695–5704. <https://doi.org/10.1158/1078-0432.CCR-10-3420> PMID: [21791632](https://pubmed.ncbi.nlm.nih.gov/21791632/)
23. Delling U, Brehm W, Ludewig E, Winter K, Julke H (2015) Longitudinal evaluation of effects of intra-articular mesenchymal stromal cell administration for the treatment of osteoarthritis in an ovine model. *Cell Transplant* 24: 2391–2407. <https://doi.org/10.3727/096368915X686193> PMID: [25581789](https://pubmed.ncbi.nlm.nih.gov/25581789/)
24. Baddoo M, Hill K, Wilkinson R, Gaupp D, Hughes C, et al. (2003) Characterization of mesenchymal stem cells isolated from murine bone marrow by negative selection. *J Cell Biochem* 89: 1235–1249. <https://doi.org/10.1002/jcb.10594> PMID: [12898521](https://pubmed.ncbi.nlm.nih.gov/12898521/)
25. Wang Y, Yu D, Liu Z, Zhou F, Dai J, et al. (2017) Exosomes from embryonic mesenchymal stem cells alleviate osteoarthritis through balancing synthesis and degradation of cartilage extracellular matrix. *Stem Cell Res Ther* 8: 189. <https://doi.org/10.1186/s13287-017-0632-0> PMID: [28807034](https://pubmed.ncbi.nlm.nih.gov/28807034/)
26. Gordon S (2003) Alternative activation of macrophages. *Nat Rev Immunol* 3: 23–35. <https://doi.org/10.1038/nri978> PMID: [12511873](https://pubmed.ncbi.nlm.nih.gov/12511873/)
27. Stein M, Keshav S, Harris N, Gordon S (1992) Interleukin 4 potently enhances murine macrophage mannose receptor activity: a marker of alternative immunologic macrophage activation. *J Exp Med* 176: 287–292. <https://doi.org/10.1084/jem.176.1.287> PMID: [1613462](https://pubmed.ncbi.nlm.nih.gov/1613462/)

28. Mosser DM, Edwards JP (2008) Exploring the full spectrum of macrophage activation. *Nat Rev Immunol* 8: 958–969. <https://doi.org/10.1038/nri2448> PMID: 19029990
29. Galleu A, Riffo-Vasquez Y, Trento C, Lomas C, Dolcetti L, et al. (2017) Apoptosis in mesenchymal stromal cells induces in vivo recipient-mediated immunomodulation. *Sci Transl Med* 9.
30. Lu W, Fu C, Song L, Yao Y, Zhang X, et al. (2013) Exposure to supernatants of macrophages that phagocytized dead mesenchymal stem cells improves hypoxic cardiomyocytes survival. *Int J Cardiol* 165: 333–340. <https://doi.org/10.1016/j.ijcard.2012.03.088> PMID: 22475845
31. Daghestani HN, Pieper CF, Kraus VB (2015) Soluble macrophage biomarkers indicate inflammatory phenotypes in patients with knee osteoarthritis. *Arthritis Rheumatol* 67: 956–965. <https://doi.org/10.1002/art.39006> PMID: 25544994
32. Kraus VB, McDaniel G, Huebner JL, Stabler TV, Pieper CF, et al. (2016) Direct in vivo evidence of activated macrophages in human osteoarthritis. *Osteoarthritis Cartilage* 24: 1613–1621. <https://doi.org/10.1016/j.joca.2016.04.010> PMID: 27084348
33. Bondeson J, Blom AB, Wainwright S, Hughes C, Caterson B, et al. (2010) The role of synovial macrophages and macrophage-produced mediators in driving inflammatory and destructive responses in osteoarthritis. *Arthritis Rheum* 62: 647–657. <https://doi.org/10.1002/art.27290> PMID: 20187160
34. Schelbergen RF, van Dalen S, ter Huurne M, Roth J, Vogl T, et al. (2014) Treatment efficacy of adipose-derived stem cells in experimental osteoarthritis is driven by high synovial activation and reflected by S100A8/A9 serum levels. *Osteoarthritis Cartilage* 22: 1158–1166. <https://doi.org/10.1016/j.joca.2014.05.022> PMID: 24928317
35. Muehe AM, Feng D, von Eyben R, Luna-Fineman S, Link MP, et al. (2016) Safety Report of Ferumoxytol for Magnetic Resonance Imaging in Children and Young Adults. *Invest Radiol* 51: 221–227. <https://doi.org/10.1097/RLI.0000000000000230> PMID: 26656202
36. Jasmin, de Souza GT, Louzada RA, Rosado-de-Castro PH, Mendez-Otero R, et al. (2017) Tracking stem cells with superparamagnetic iron oxide nanoparticles: perspectives and considerations. *Int J Nanomedicine* 12: 779–793. <https://doi.org/10.2147/IJN.S126530> PMID: 28182122
37. Theruvath AJ, Nejadnik H, Lenkov O, Yerneni K, Li K, et al. (2019) Tracking Stem Cell Implants in Cartilage Defects of Minipigs by Using Ferumoxytol-enhanced MRI. *Radiology*: 182176.